

JEAI-26-45

Bending Angle Influence of Grain-Oriented Silicon Steel on Iron Loss and Domain Patterns

Hisashi Mogi*, Takahito Mizumura and Masaru Takahashi

Steel Research Laboratories, Nippon Steel Corporation, Futtsu, Chiba, Japan

*Corresponding author: Hisashi Mogi, Steel Research Laboratories, Nippon Steel Corporation, Futtsu, Chiba, Japan, E-mail: mogi.dg3.hisashi@jp.nipponsteel.com

Received date: February 03, 2026; Accepted date: February 16, 2026; Published date: March 05, 2026

Citation: Mogi H, Mizumura T, Takahashi M (2026) Bending Angle Influence of Grain-Oriented Silicon Steel on Iron Loss and Domain Patterns. J Eng Artif Intell Vol.2 No.1: 45.

Abstract

Bending angle influence of grain-oriented silicon steel on the iron loss and domain patterns was evaluated. The results showed that the additional bending at the octagonal wound core corner made more losses, when the initial plastic bending angle was several degrees apart from the designed angle. The iron loss in the octagonal wound core increased 31 % when the initial plastic angle was 10° apart from the designed angle. At that bending angle, the magnetic domains were easily saturated and elastic stress was widely distributed near the bending corner.

Therefore, it needs to avoid the additional bending at the core corner or to achieve the exact 45° bending angle equal to the designed angle.

Keywords: Bending angle; Domain patterns; Grain-oriented silicon steel; Iron loss; Elastic strain; Plastic strain

Introduction

The Grain-Oriented Silicon Steel (GOES) is a soft magnetic material and it is mainly used for transformer cores. These transformers step down the commercial voltage from 6600 V to 100~200 V as the distribution voltage. These are called distribution transformers, which are made as the shape of wound cores. The wound cores are mostly formed as TRANCO-type cores, which is deformed to the ellipse and finally to the near-rectangular shape by plastic forming and the core is annealed at 800 °C in the furnace to relief the stress.

On the other hand, recently octagonal wound cores [1,2] gradually spread in the distribution transformers. With this core, the GOES is 45° bent one by one and stacked and formed as octagonal shape. Since the high efficiency is required for the transformers, it must have low iron loss. The iron loss is influenced by the stress, which is induced by forming wound cores, shearing the sheets and binding the laminations. Particularly, bending the GOES is unique process because it makes the plastic and elastic strain transversely across the magnetic circuit [3,4], especially, at small curvature radius. In that process, the stress is one of the deteriorate elements for the iron loss in the cores.

The octagonal wound core sheet is 45° bent at the eight corners, however, the angle of each corner is fluctuated substantially. When this angle is apart from the designed angle 45°, the space is formed between the core laminations, which depends on the deviation from the designed angle. Consequently, this applies the stress concentrating to the corners, which makes the iron loss increase. Therefore, it needs to evaluate the iron loss on this phenomenon precisely.

To evaluate the statistical distribution of the bending angle in the octagonal wound core, the 12 GOES sheets are measured, where one sheet has 8 angles, so the measured angles totally come to 96. The samples belong to 23 ZH and 20 ZDKH. In this statistical data the average angle is 43.8° and standard deviation is 1.53°. The highest frequent angle is 45° and the angles of less than 44°, also exist as some amounts. On the other hand, the angles more than 46° hardly exist, because the angle is controlled to make the designed angle of 45°, but all of the corners do not have exact 45°. This distribution is caused by the spring back of the GOES sheet after the bending.

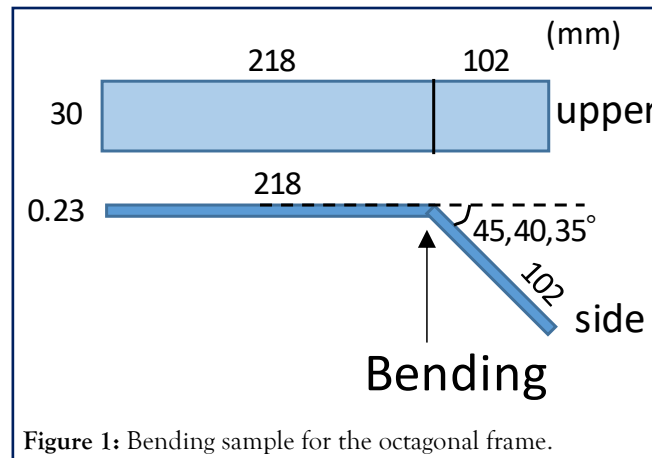
In this work, the bending angle influence on the iron loss is evaluated and discussed, which is caused by the spring back of the GOES sheet by the adjustment force to fit along the core frame. And to understand the phenomenon, the applied stress and the strain is analyzed by FEM and observe the magnetic domain patterns.

Experimental Procedure

Bending of the samples

Samples used in this work are GOES sheets with the thickness of 0.23 mm. The samples are bent at 35° to 45°. **Figure 1** shows a bending sample made of 23 ZH. This sample

is commercially used as 30 mm wide and 320 mm long Epstein shape. The samples are bent by the 2,000 kN servo-press which has the L-shaped jig attached to that punch. The curvature radius R of the die edge is 1 mm and the punch edge is R=5 mm. The clearance between die and punch is 0.3 mm and the forming velocity is 75 mm/sec, which is almost the same velocity to form the practical octagonal wound core. The bending corner is formed at the 102 mm apart from the sample edge. The bending angles are 35°, 40° and the 45° which is the designed angle of the practical octagonal wound cores. To fit the bending samples along the octagonal frame, the additional bending angle 0°, 5°, 10° are respectively needed.



The bending angle is controlled by a descent height of the servo-press punch. The higher descent height is settled, the smaller bending angle is obtained. Although the servo-press is for large forming use and not for small samples, the accuracy of the angle is 0.7~1.0° as the standard deviation.

The obtained bending angle is 44.4° then at the descent height of 527.0 mm, 40.4° at 526.6 mm and 35.9° at 526.0 mm, respectively. So, the samples which have 5° interval, the bending corner of R=1.4 mm are obtained.

These 8 pieces of bending samples are fit along the octagonal frame to make the continued magnetic path and the iron losses are measured.

Evaluation of the samples with the octagonal frame

The above mentioned octagonal wound core which consists of 8 Epstein pieces of 30 mm x 320 mm is measured. The experimental procedure is shown in **Figure 2**. First, to distinguish the strain caused by both plastic bending and additional elastic bending at the bending corner of GOES, the samples are annealed at 800 °C in 4 hours, then the elastic strain caused by the plastic bending is eliminated. Next, the 8 pieces of bending samples are assembled and fit along the octagonal frame to form a core. The octagonal frame is made of a Bakelite, which supports the bending samples covered from outside and along the side guides.

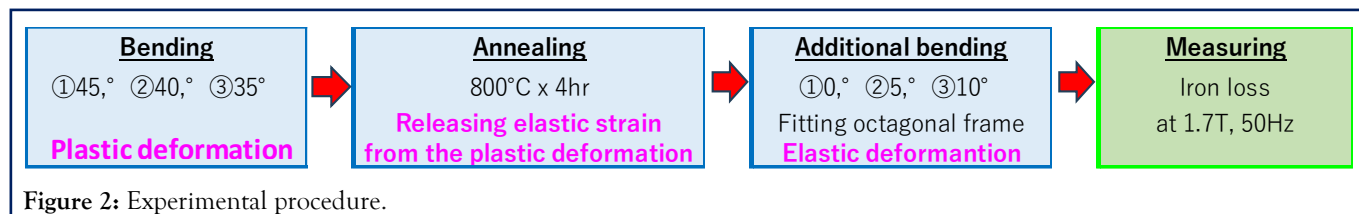


Figure 3 displays the octagonal frame and the samples. In the case of 45° of the bending angle, since the sample is fit the

frame well, the additional bending angle on the frame is ① 0°. Decreasing the bending angle increases. In other words, the

additional bending angle depends on the clearance apart from the frame. In the case of 40° of the bending angle, the

additional bending angle is ② 5°, in the same way, at 35° of the bending angle, the additional bending angle is ③ 10°.

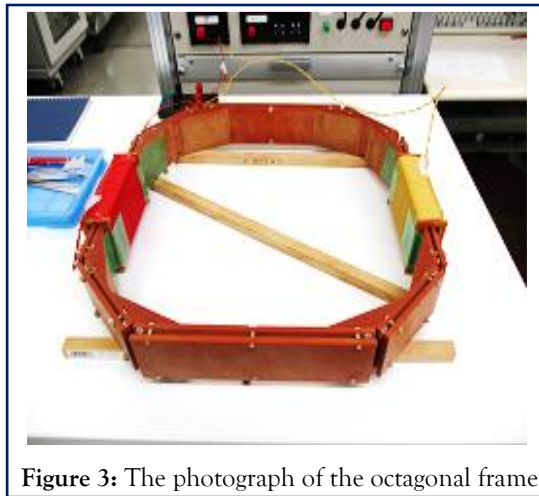


Figure 3: The photograph of the octagonal frame.

In Figure 4, the octagonal frame on the samples is presented as the green color and the blue-colored bending samples are fit along this frame one by one. The octagonal frame consists of 220 mm sides and 100 mm sides which are arranged alternately. 4 pieces of bending samples are put along the frame make 4 places of gaps. When one more layer of the samples as the second is stacked on them, the second layer gaps are avoided to be on the same places of the first layer, so that most of the magnetic fluxes flow through the inner samples, not to stray out of them.

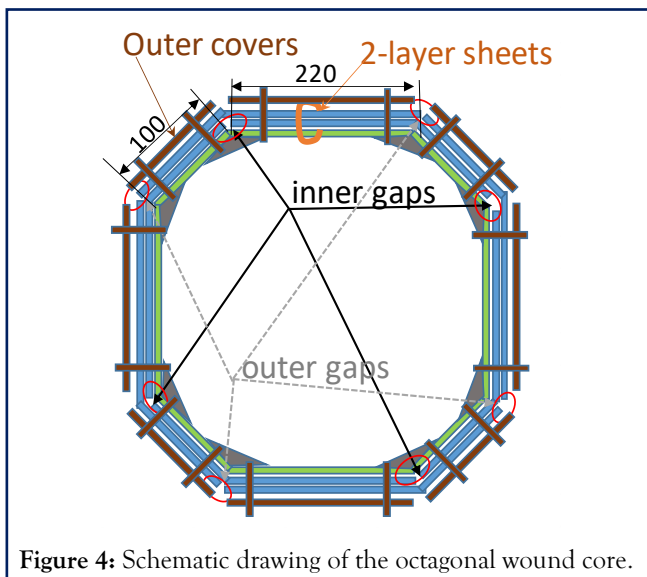


Figure 4: Schematic drawing of the octagonal wound core.

Red and yellow windings are for the excitation and they supply the magnetic flux into the octagonal wound core. The second winding to measure the flux density and the iron loss is placed on the linear portion of the frame. Finally, the induced voltage is measured with the digital oscilloscope, Yokogawa DL750 and it calculates the iron losses.

Experimental Results

Table 1 shows the iron losses which depend on the additional bending angles of the samples fit along the octagonal frame. The flux density of the double-layered core is 0.85 T and the one-layered bending sample without gap at the corner is 1.7 T. Then, at the additional bending angle, 0°, where there is no elastic bending, the iron loss is 0.290 W/kg. At 5° the iron loss is 0.328 W/kg, since the compression stress by the outer covers is applied to the samples. At 10° the iron loss is 0.380 W/kg, which increases 31 %, compared to the one at 0°.

Table 1: Additional bending angles and iron losses (0.85T).

Bending angle (°)	0	5	10
Hysteresis loss (W/kg)	0.147	0.150	0.201
Eddy current loss (W/kg)	0.143	0.178	0.179
Iron/Total loss (W/kg)	0.290	0.328	0.380

Hysteresis losses also increase in the increase of the additional bending angle. This is because the elastic strain generated by the additional bending makes magnetic flux flow disturbed and decreases the permeability and increases the excitation currents. The hysteresis loss increases 37 % at 0°, compared to the one at 5°. Eddy current losses also increase 25 %. This is because in-plane eddy current generates caused by the flux intersection between the sample layers and generation of closure domains. Moreover, before annealing, the iron losses with the plastic and elastic strains are 0.310 W/kg at 0°, 0.340 W/kg at 5°, 0.396 W/kg at 10°, respectively and it is clear that the iron losses before annealing are 4-10 % larger than ones after annealing.

Results and Discussion

Plastic and elastic strain distribution

Based on this experimental result, it is considered that the plastic and the elastic stresses each by the bending must be separated on the iron loss influence. Therefore, the bending stress distribution is analyzed on the finite element method with the strain calculation solver, LS-DYNA R14.1.0. Both plastic and elastic analyses are applied 2-dimensionally, to the core cross section divided into 11 layers. The material parameters are normal GOES values, which are 7.65g/cm² as the density, 122.45x10³ as the Young's modulus, 0.368 as Poisson ratio.

In the plastic bending the stress is calculated based on the work hardening law as the equation (1).

$$\bar{\sigma} = C (\bar{\epsilon}^p + \epsilon_0)^{n^*} \quad (1)$$

Where, C is the constant of 451.2 MPa, ϵ_0 is the strain multiplier of 0.0298 and n^* is the work hardening coefficient of 0.027, respectively.

Figure 5 displays the calculation results of plastic and elastic strains by the bending before annealing. In the longitudinal direction of the surface, there are two strong plastic strains within the 1 mm near the bending corner in Figure 5a. These strains presumably affect the decrease of surface permeability and the increase of hysteresis loss. On the other hand, the elastic stress distributes the inner cross section and is firmly affected by the plastic strain in Figure 5b. In this figure, the tensile stress is at the outer boundary of the core and the compressive stress is at the internal boundary, respectively and the strength is both 300 MPa.

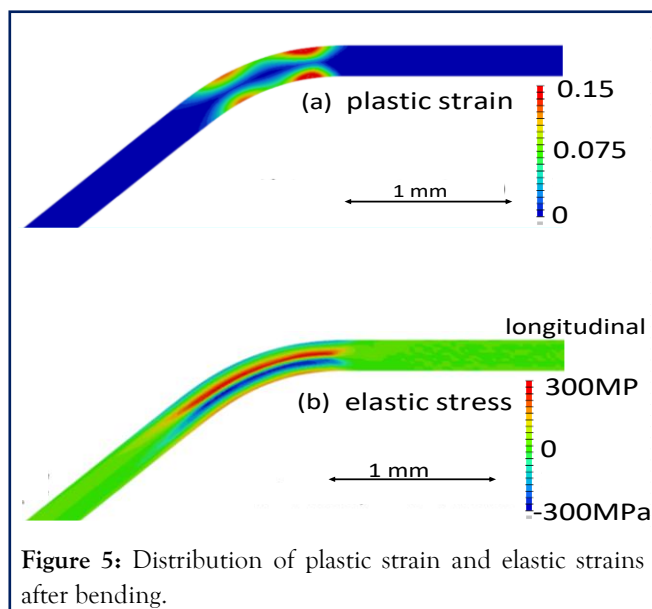


Figure 5: Distribution of plastic strain and elastic strains after bending.

Next, the additional bending stress distribution is calculated, where it is annealed to eliminate the inner elastic strains in Figure 6a. No elastic stress cannot be seen here, but applying additional bending, the elastic strain is distributed. Increasing the bending angle, the stress area expectedly expands and at 10° of additional bending, 300 MPa stress is distributed in the range of about 5 mm from the bending corner in the Figure 6b. Therefore, compared the beginning plastic bending, the elastic stress is more widely distributed in the Figure 6c. This is the reason that it increases the iron loss with 31 % and the hysteresis loss with 38 %.

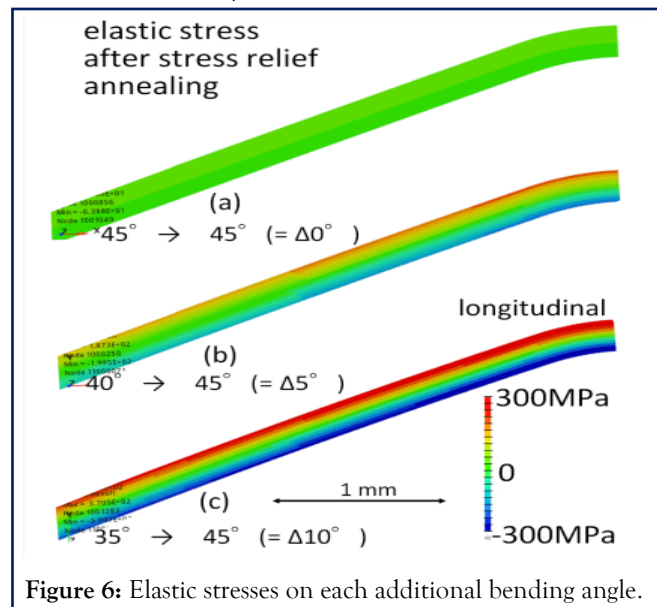


Figure 6: Elastic stresses on each additional bending angle.

Magnetic domain observation

The material structure which mostly affects the iron loss is magnetic domains. The magnetic domains near the bending corner are observed by scanning electron microscope, JEOL JEM-Z2100BMG in the internal sample surface and by the Faraday effect in the magneto-optical sensor, Matesy Cmos-magview XL in the outer sample surface, respectively. In the scanning electron microscope, since the electron beam is irradiated to the internal side of the sample surface, the domain patterns in the internal side surface can be obtained. On the other hand, with the Cmos-magview, since the domains patterns are observed through the fixed bottom sensor, the outer side of the domains pattern is obtained.

After bending and annealing, at the corner from the internal surface, 180° wall can be seen clearly, the plastic stress influence cannot be seen in Figure 7. Therefore, the plastic strain in the range of 1 mm at the corner and the elastic strain distributed in the inner core in Figure 5 do not affect these surface domain patterns.

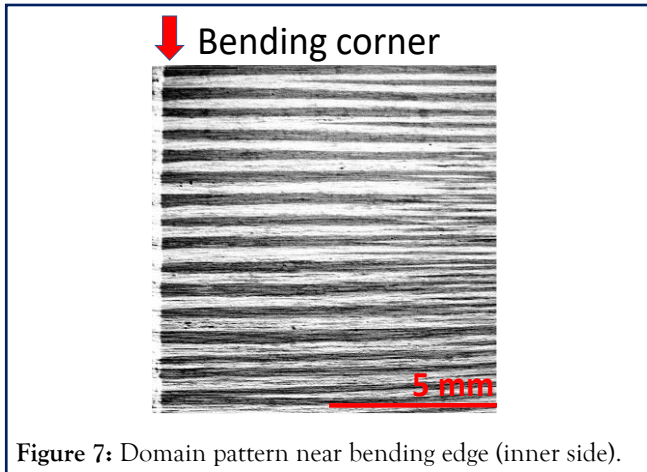


Figure 7: Domain pattern near bending edge (inner side).

At the outer surface the remarkable domain pattern disturbance cannot be seen near the bending corner in **Figure**

7, at the flux density of 0 T. According to the FEM of stress distribution, although the 300 MPa elastic stress is distributed only 10 % on the surface, the other 90 % in the center is no stress. Therefore, it is expected that the closure domains which occur by the applied force cannot generate, then the 180° walls exist stably.

However, when DC magnetic field at 30 A/m ($\sim 0.8T$) are applied, the domains start saturating from the bending corner. The larger the angle of bending is, the more the saturated domain area is. Therefore, under the excitation, the influence of bending stress is clearly observed, so that the iron losses expectedly increase. Especially, in the case of 10°. At the excitation of 0.46 T near the bending corner, it is confirmed that the domains are saturated in **Figure 8**.

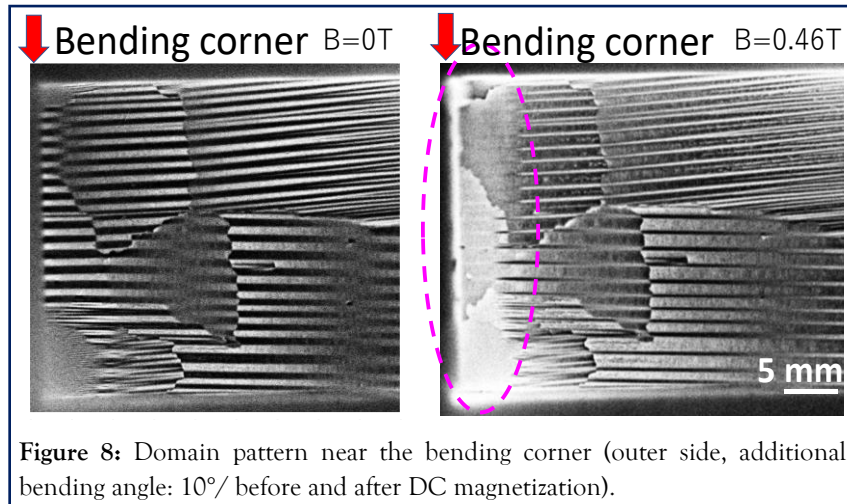


Figure 8: Domain pattern near the bending corner (outer side, additional bending angle: 10°/ before and after DC magnetization).

Figure 9 shows that the DC excitation field and the saturation area of domains are correlated. Applying the DC

field, domain pattern is saturated at the bending corner and saturation area is gradually increasing.

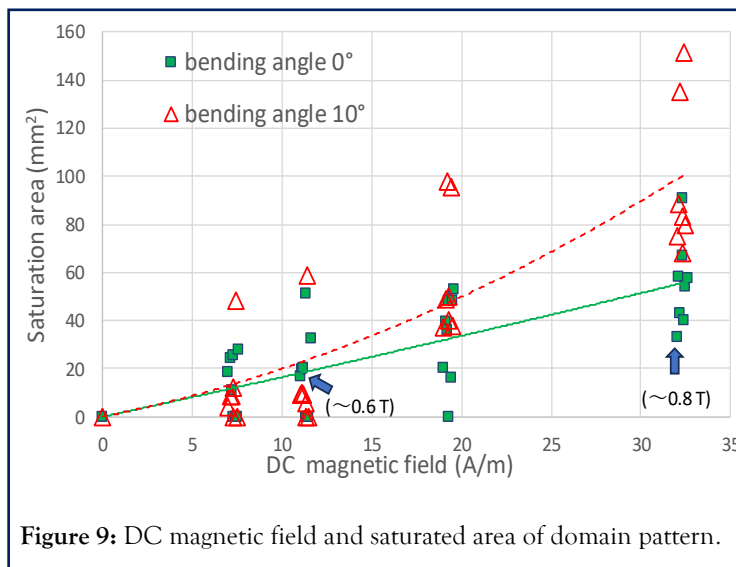


Figure 9: DC magnetic field and saturated area of domain pattern.

This tendency is clear at the additional bending angle of 10° . This increase of the additional bending angle from 0° to 10° is statistically more remarkable when the stress distribution is wider. Therefore, the result shows the additional bending makes more losses and this reason is expectedly the magnetic domain saturation at the bending corner. Consequently, to avoid the iron loss increase in the octagonal wound cores, it needs to achieve the exact 45° designed angle at the corner without the additional bending.

Conclusion

Bending angle influence of grain-oriented silicon steel on the iron loss and domain patterns was evaluated. The results showed that the additional bending at the octagonal wound core corner made more losses, when the initial plastic bending angle was several degrees apart from the designed angle.

- The iron loss in the octagonal wound core increased 31 % when the initial plastic angle was 10° apart from the designed angle.

- At that bending angle, the magnetic domains were easily saturated and elastic stress was widely distributed near the bending corner.
- Therefore, it needs to avoid the additional bending at the core corner or to achieve the exact 45° bending angle equal to the designed angle.

References

1. Hagihara H, Takahashi Y, Fujiwara K, Ishihara Y, Matsuda T (2014) Magnetic properties evaluation of grain-oriented electrical steel sheets under bending stress. *IEEE Trans on Mag* 50: 1-4. [Crossref], [Google Scholar]
2. Hernandez I, Olivares-Galvan JC, Georgilakis PS, Canedo JM (2010) A novel octagonal wound core for distribution transformers validated by electromagnetic field analysis and comparison with conventional wound core. *IEEE Trans on MAG* 46: 1251-2485. [Crossref], [Google Scholar]
3. Pfützner H, Futschik K and Luo Y (1982) Effect of bending on G.O. silicon iron sheets. *IEEE Trans on MAG* 18: 1499-1501. [Crossref], [Google Scholar]